

1. Introduction

Laser-driven proton beams have significant application potential in areas such as radiation therapy, radiobiology, and fusion ignition. However, laser-driven proton beams are characterized by a broad energy spectrum, short pulses (~ps), and high transient flux, making it challenging to quickly and accurately diagnose the parameters of such proton beams.

To achieve simultaneous online diagnostics of both the energy spectrum and spatial distribution of laser-driven proton beams, we propose a proton spectrometer based on scintillation fibers, which consists of a scintillation fiber component and two imaging systems. Using the quasi-monoenergetic proton beam produced by the synchrotron accelerator, we calibrated the spectrometer and demonstrated its capability to resolve 1D energy spectrum of a quasi-monoenergetic beam with spatially non-uniform distribution.

2. Design of the spectrometer

- ◆ The scintillation-fiber-cube spectrometer (SFCPS) consists of a scintillating fiber cube and two imaging systems.
- ◆ The scintillating fiber cube is composed of an interleaved arrangement of 120 mutually orthogonal scintillating fiber (SF) arrays. The diameter of the SF is 0.5 mm.
- ◆ The imaging system comprises a lens, CCD, and several optical filters.
- ◆ The focal length of the lens is 25 mm, and the F-number ranges from 2 to 16.
- ◆ SFs with a circular cross-section have better photon transmission efficiency.

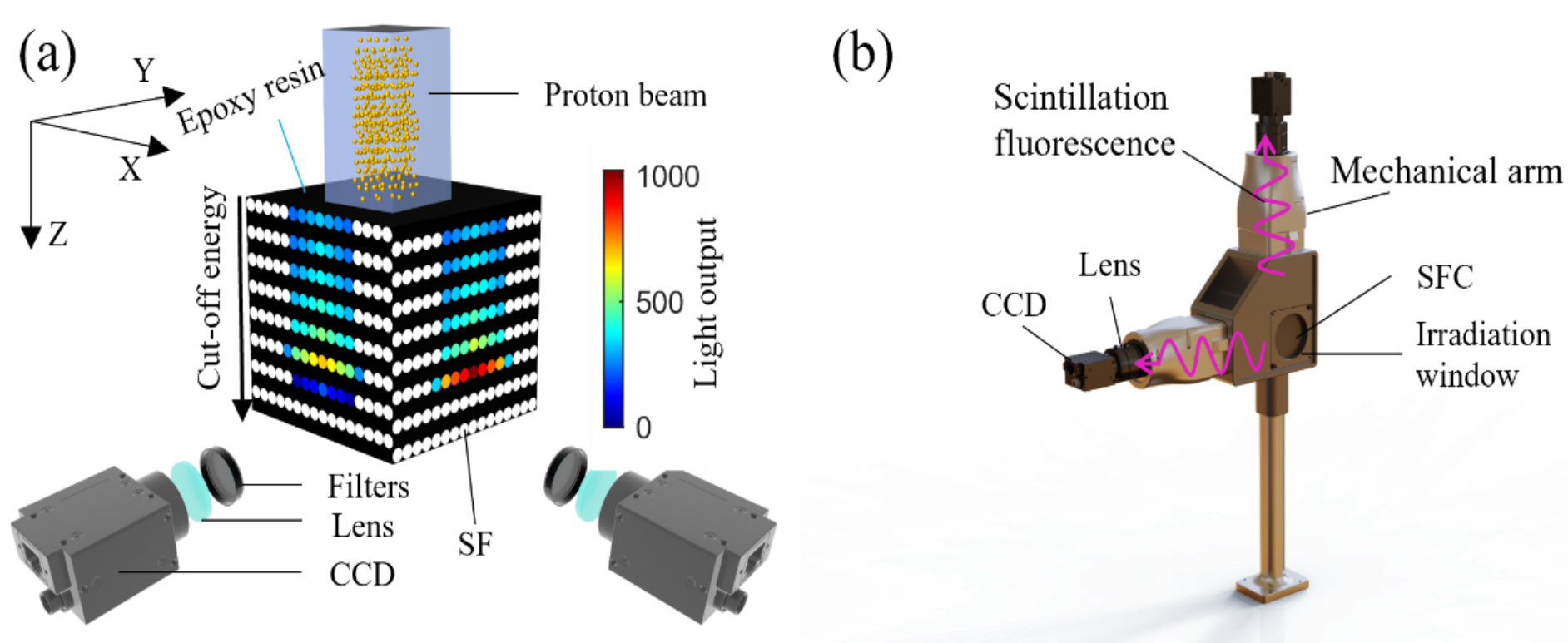


Fig.1 (a) Schematic diagram of SFCPS detection. (b) Mechanical assembly diagram of the SFCPS with an aluminum alloy housing.

3. Detection principle

- Protons deposit energy in the scintillation fiber, leading to the emission of visible light. The intensity of the light output is related to the energy and dose of the protons.
- The light output intensity detected by the spectrometer is proportional to the initial generated light output intensity, with a proportionality constant denoted as K. K is referred to as the response coefficient.
- With the Monte Carlo software Geant4, we calculated the light output response of the spectrometer for different proton energies, as shown in Fig. 2a, which provides the necessary data foundation for Retrieving the proton energy spectrum.
- The energy measurement range of the spectrometer is 6-93 MeV (see Fig.2b), with an energy resolution of 0.5% at 80 MeV.

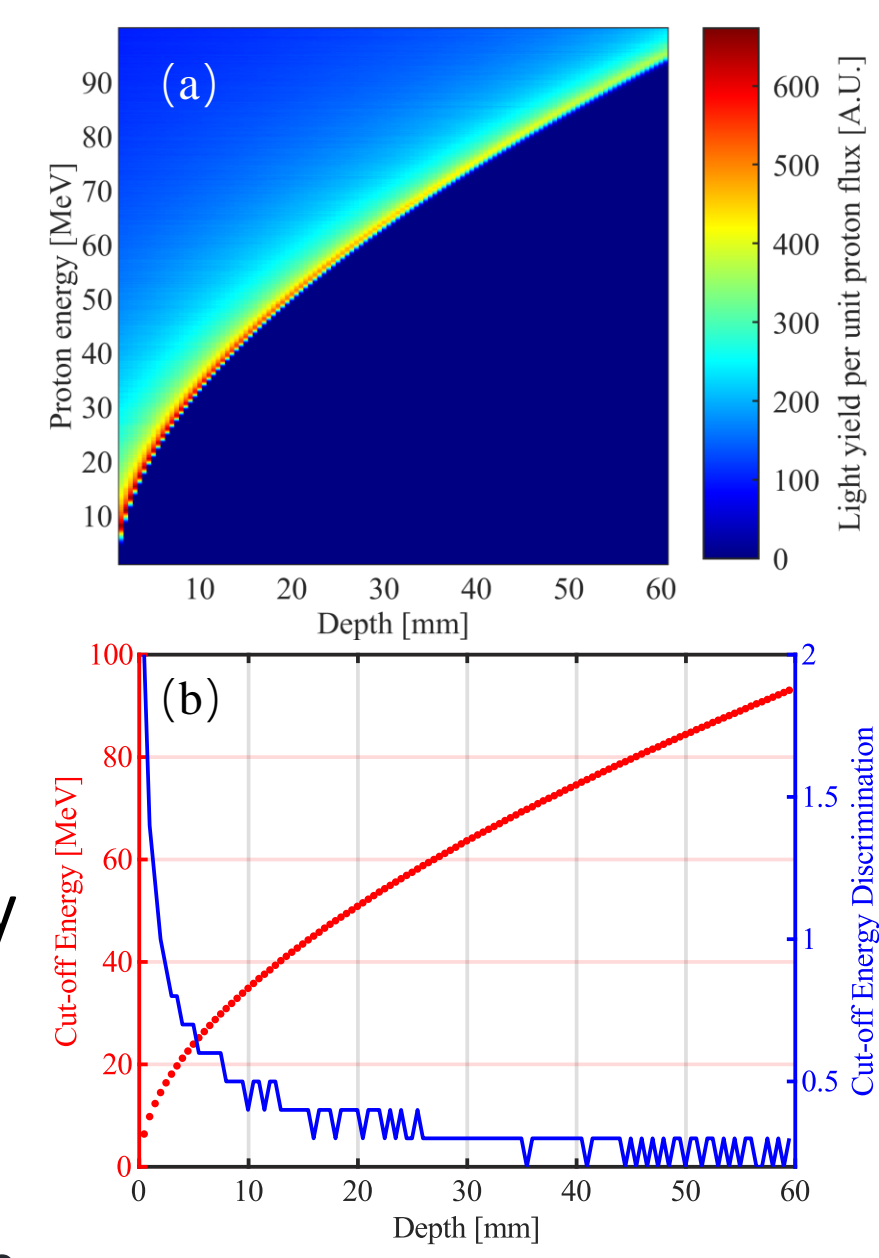


Fig2. (a) The light output response of SFs at different depths in the SFC as a function of proton energy. PLD refers to proton line density. (b) The cut-off energy and the uncertainty in cut-off energy estimation for SFs at different depths in the SFC, obtained through Monte Carlo simulation.

4. Proton energy spectrum reconstruction method

For a parallel proton beam, the specific spectrum reconstruction method is shown in Fig.3. The light output of the SF array along the Z direction at position x_k is mainly related to the beam energy spectrum at that position. Thus, the light output curve at position x_k along the Z direction can be extracted, and the energy spectrum $f(E, x_k)$ at position x_k can be retrieved by using the least-squares method, with the mean square error (MSE) function given by:

$$MSE_{x_k} = \frac{1}{M(x_k)} \sum_j \left(\int_0^{E_{cut}(x_k)} f(E, x_k, \epsilon^{x_k}) R_{LD}^j(E) / n_j dE - \overline{KY_G^j} \right)^2 \quad (1)$$

where $M(x_k)$ represents the number of SFs emitting light at position x_k , $E_{cut}(x_k)$ is the cut-off energy of the proton beam at position x_k , $R_{LD}^j(E)$ represents the proton line density light output response function of the jth SF, n_j and $\overline{KY_G^j}$ represent the number of pixels and average grayscale value of the light output image, respectively. ϵ^{x_k} is the parameter space to be retrieved for the proton energy spectrum $f(E, x_k, \epsilon^{x_k})$ at position x_k .

The Levenberg-Marquardt algorithm can be used to retrieve this least-squares problem, with the iterative formula at the $(n+1)$ th iteration given by:

$$\epsilon_{n+1}^{x_k} = \epsilon_n^{x_k} - (H + \alpha I)^{-1} \nabla MSE(\epsilon_n^{x_k}) \quad (2)$$

where H is the Hessian matrix of $MSE_{x_k}(\epsilon_n^{x_k})$, ∇ denotes the gradient operator, and α is the damping factor. During the iteration, if the new parameter update reduces the MSE, the damping factor is decreased; otherwise, it is increased.

The unit of $f(E, x)$ mentioned above is the number of protons per unit length and per unit energy. In order to obtain the proton energy spectrum of unit flux and unit energy, the 1D transverse profile size of the XOZ plane can be used to obtain it:

$$F(E, x) = \frac{f(E, x)}{Y_{FWHM}} \quad (3)$$

where Y_{FWHM} is the full width at half maximum (FWHM) of the 1D lateral profile of the light output in the YOZ plane.

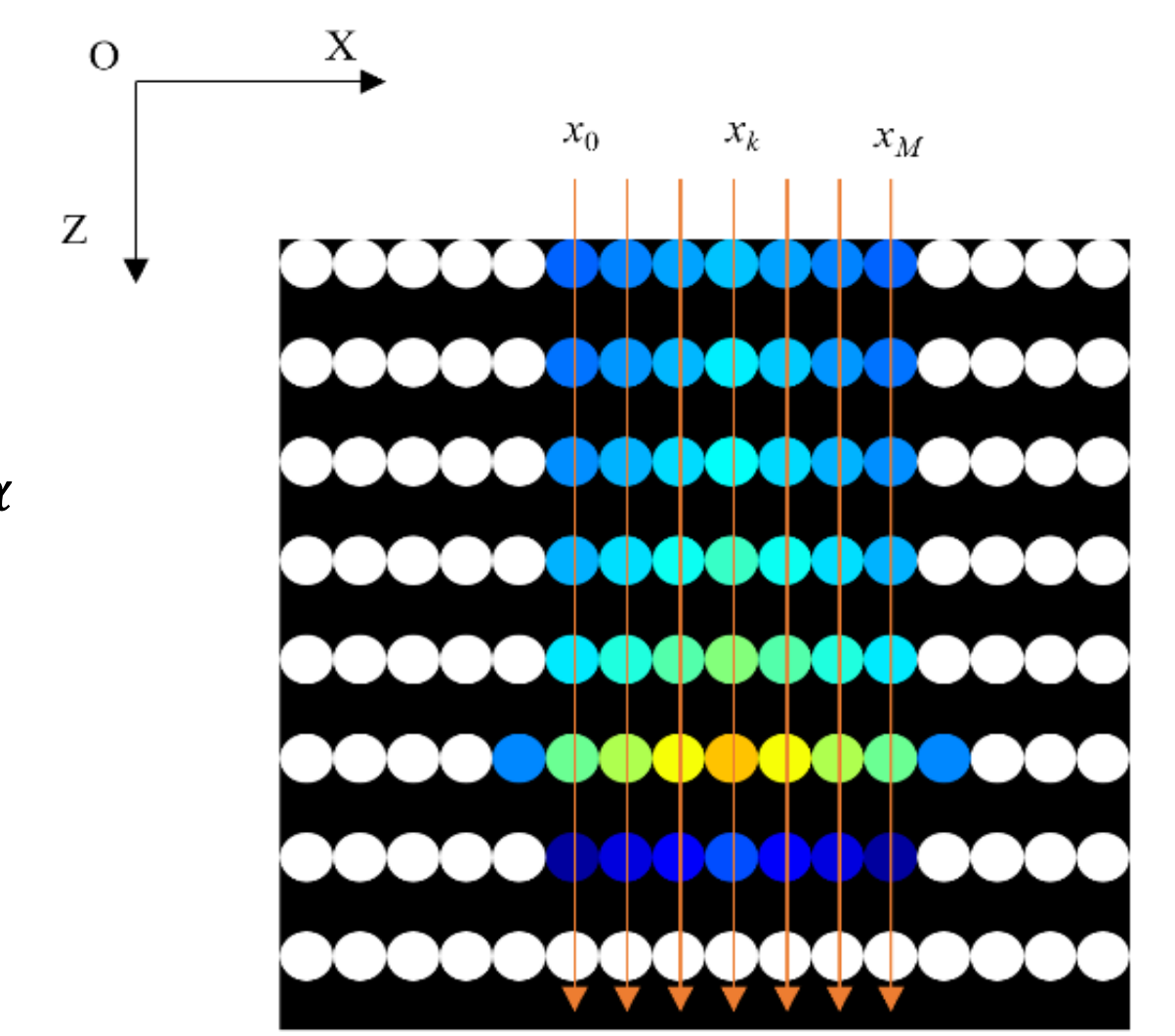


Fig.3 Spectral reconstruction scheme for a parallel and vertically incident beam

5. Calibration Experiment

5.1 Experimental Setup

The experiment was conducted at the irradiation platform of the Xi'an 200 MeV Proton Application Facility (see Fig. 4a).

- Experimental Objective: Absolute particle number calibration of the spectrometer.
- Beam Parameters: Energy 80 MeV, flux 2×10^8 p/cm².
- Size of the square collimator: 10 mm.
- Detector Setup: The lens F-number is set to 2, and the SFCPS is equipped with an iron shielding shell to minimize radiation exposure to the CCD chip.

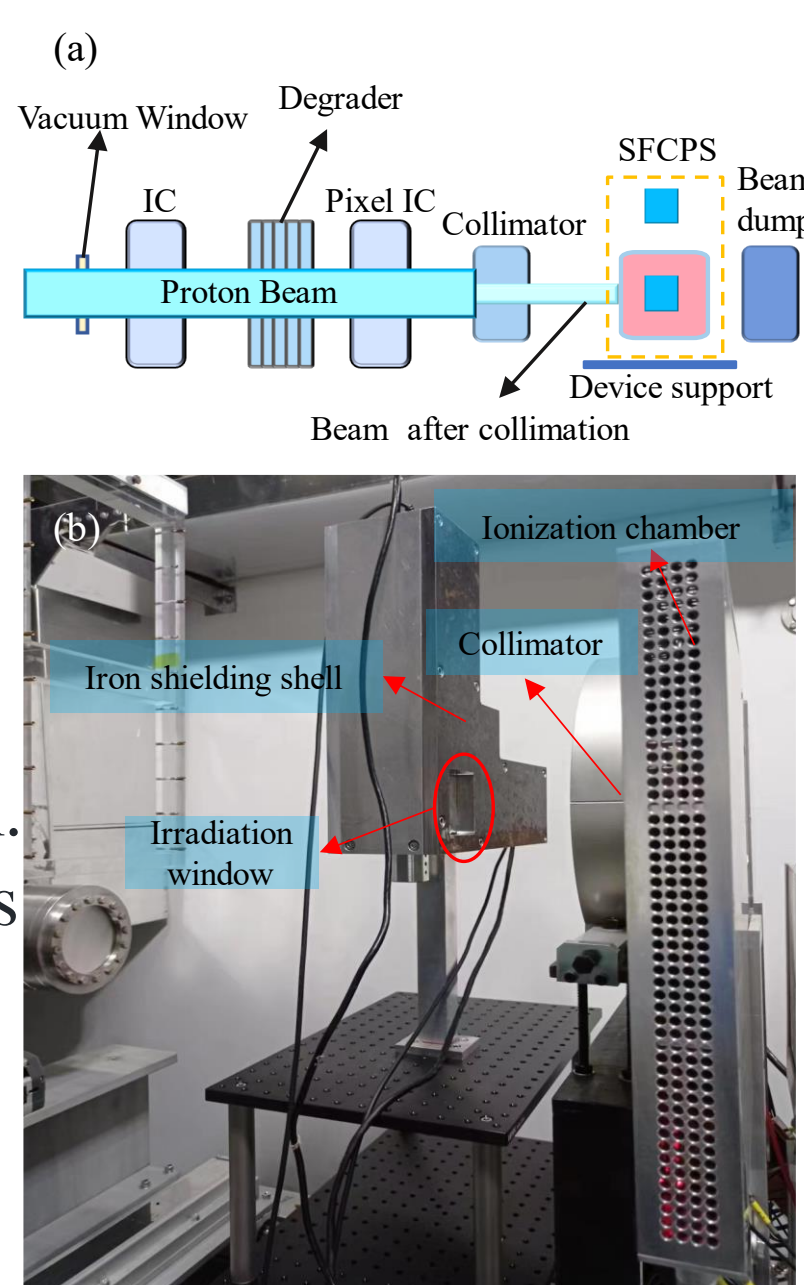


Fig. 4 (a) Schematic diagram of the experimental terminal. (b) The SFCPS with an iron shielding shell, is placed behind the collimator.

5.2 Results

- The light output distribution on the XOZ and YOZ planes of the SFCPS is shown in Fig. 5a and 5b.

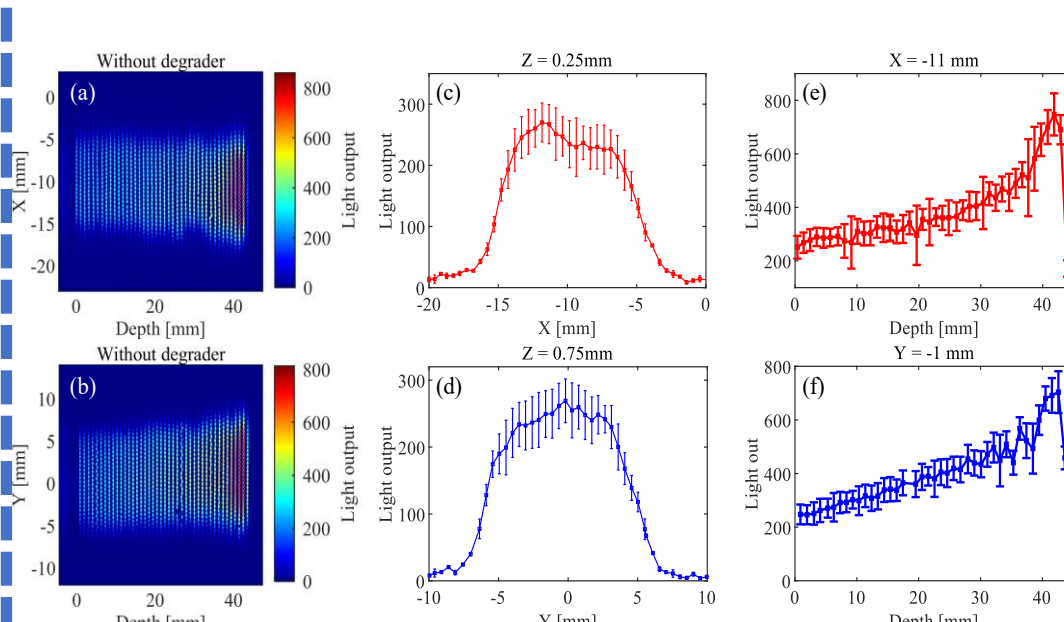


Fig.5 Spatial distribution of light output in the XOZ plane (a) and the YOZ plane (b). Lateral light output distribution of the SFC at Z=0.25 mm in the XOZ plane (c) and at Z=0.75 mm in the YOZ plane (d). Longitudinal fiber array light output distribution at X=-11 mm in the XOZ plane (e) and at Y=-1 mm in the YOZ plane (f).

- From the 1D transverse profile of the light output, it can be observed that the uniformity of the beam in the X direction is somewhat poorer.
- The longitudinal light output profile exhibits a Bragg peak shape.

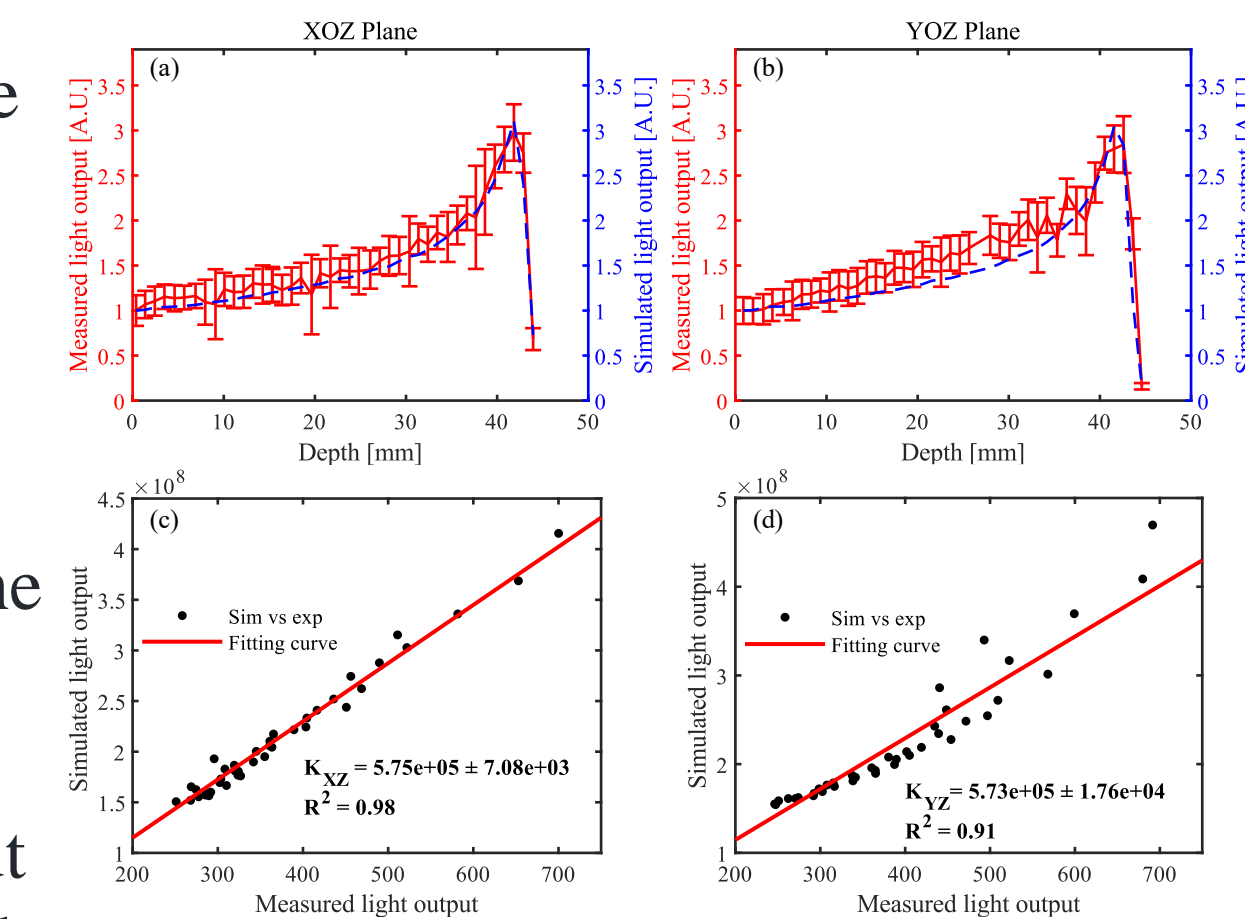


Fig.6: Normalized curves of the light output detected in the XOZ plane (a) and YOZ plane (b) compared to the simulated light output. Fit curves of experimental (exp) versus simulated (sim) light output in the XOZ plane (c) and YOZ plane (d). The red line represents the proportional curve. K_{XZ} and K_{YZ} correspond to the response factors of the SFCPS in the XOZ and YOZ planes.

- The detected light output is consistent with the simulation results.
- The response coefficient K of the spectrometer obtained from linear fitting is approximately 5.7E5.

6. Application of the SFCPS

1D Energy Spectrum Reconstruction

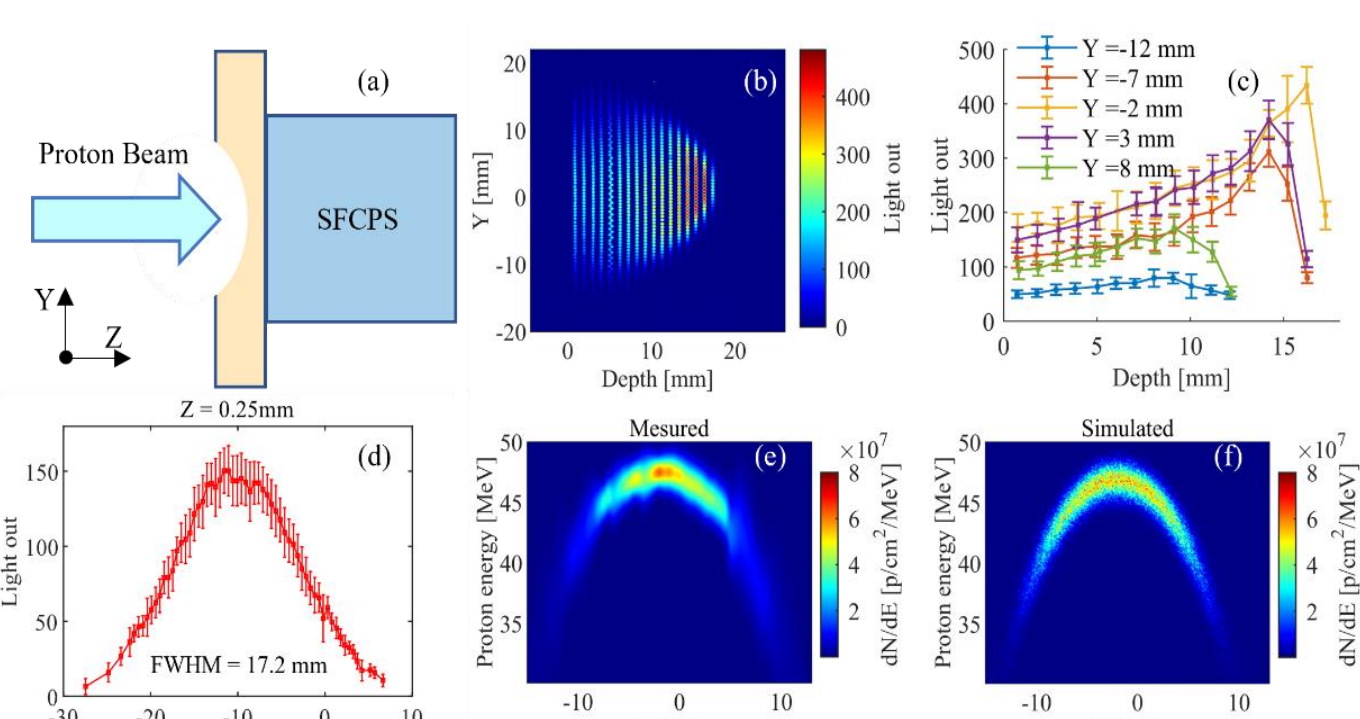


Fig.7 (a) Schematic of the proton beam irradiating the SFCPS after being modulated by a special degrader. (b) Symmetrical peak distribution of scintillation fluorescence in the YOZ plane. (c) Longitudinal SF array light output distributions extracted at different Y positions. (d) 1D lateral profile of the proton beam in the X direction. (e) Retrieved mean 2D energy spectrum distribution of the proton beam in the Y direction at the SFC. (f) Simulated mean energy spectrum distribution of the proton beam in the Y direction at the SFC.

- Using a specially shaped degrader, a spatially non-uniform broad energy spectrum proton beam is obtained. To restore the energy spectrum, the energy spectrum distribution of the beam must be known in advance.
- The one-dimensional energy spectrum of the beam is reconstructed using the energy spectrum reconstruction algorithm described previously, and the restored energy spectrum results are consistent with the simulation

7. Conclusion

- The energy range of the spectrometer is 6 MeV - 93 MeV, with an energy resolution of 0.5% at 80 MeV.
- The spatial resolution is approximately 0.5 mm.
- When the energy spectrum distribution of the beam is known, the spectrometer has the capability to reconstruct the two-dimensional energy spectrum of the spatial proton beam.

Acknowledgement

The authors sincerely thank Mr. Wang Di and Professor Sigang Wang for their assistance and discussions regarding the experimental testing.